JOURNAL OF PHYSICAL ORGANIC CHEMISTRY
J. Phys. Org. Chem. 2005; **18:** 398–407
DOI: 10.1002/poc.887

Thermo-solvatochromism of zwitterionic probes in aqueous aliphatic alcohols and in aqueous 2-alkoxyethanols: relevance to the enthalpies of activation of chemical reactions

Erika B. Tada, Priscilla L. Silva, Clarissa Tavares and Omar A. El Seoud*

Instituto de Química, Universidade de São Paulo, C.P. 26077, 05513-970 São Paulo, S.P., Brazil

Received 11 August 2004; revised 29 September 2004; accepted 05 October 2004

ABSTRACT: The thermo-solvatochromic behavior of 2,6-dichloro-4-(2,4,6-triphenylpyridinium-1-yl)phenolate (WB), 1-methylquinolinium-8-olate (QB) and 4-[2-(1-methylpyridinium-4-yl)ethenyl]phenolate (MC) was investigated in binary mixtures of water (W) and 2-alkoxyethanols (ROEtOH) in the temperature ranges from 10 to 60 °C (2-ethoxyethanol and 2-*n*-propoxyethanol) and 10 to 40 °C (2-*n*-butoxyethanol). Thermo-solvatochromic data were treated according to a model that is based on the presence *in bulk solution* of three solvents, W, ROEtOH and a 1:1 H-bonded species, ROEtOH–W. Solvation by ROEtOH–W is favored over solvation by either of the two precursor solvents. The present data, and those recently published on thermo-solvatochromism of the same probes in five alcohols (methanol, ethanol, 1-propanol, 2-propanol and 2-methyl-2-propanol) and one ROEtOH (2-methoxyethanol), were submitted to regression analysis. The results indicate that solvation is more sensitive to solute–solvent hydrophobic interactions than H-bonding between the probe phenoxy oxygen and the hydroxyl group of the H-bond donating solvent (HBD). Temperature increase results in gradual desolvation of the probes, due to the concomitant decrease of the structure of all components of the binary solvent mixture. For pure solvents, the temperature-induced desolvation depends on the structure of the probe (order: WB > MC > QB) and the HBD solvent (order: 2-ethoxyethanols > aliphatic alcohols, for the same alkyl group; organic solvent > water). The probe solvatochromic response is due to the electronic transition zwitterion → di-radical; it serves as a model for reactions that are associated with a large polarity difference between the reagents and activated complexes. For WB, for $\Delta T = 50\,^{\circ}\mathrm{C}$, the desolvation energies range from 2.1 to 3.7 kcal mol^{-1}. The contribution of temperature-induced desolvation to the activation enthalpies of these reactions is, therefore, important. Copyright © 2005 John Wiley & Sons, Ltd.
Supplementary electronic material for this paper is available in Wiley Interscience at http://www.interscience.wiley.com/jpages/0894-3230/suppmat/

KEYWORDS: thermo-solvatochromism; aqueous alcohols; aqueous alkoxyethanols; solvation energy

INTRODUCTION

The effects of reaction media on the rates and equilibria of chemical reactions are a fascinating subject. Important examples of the effects of solvents on reactivity include the spontaneous decomposition of benzisoxazole-3-carboxylate;[1] rate enhancements of many S_N2 reactions, and inversion of the order of nucleophilicity of the halide ions, as H-bond donating (HBD) solvents are replaced with non-H-bond donating (non-HBD) solvents;[2,3a] and the partial or complete control of the energetics of reactions involving neutral molecules and strongly solvated species, in particular alkoxide and hydroxide ions, by the barrier required for desolvation of the base.[4] Intensive efforts have been directed, therefore, at understanding solvation and its dependence on the properties of solutes and solvents.[3]

The study of solvatochromism has contributed a great deal to our understanding of solvation. The UV–visible spectra, absorption, or emission of certain solvatochromic substances (hereafter designated ‘probes’) were measured in solvents and/or solvent mixtures, and the data therefrom have been employed to analyze both solvent–probe and solvent–solvent interactions.[3b] Extensive use has been made of an empirical solvent polarity scale, E_T, calculated from

$$E_T\,(\mathrm{kcal\,mol^{-1}}) = 28591.5/\lambda_{\max}(\mathrm{nm}) \qquad (1)$$

which converts the electronic transition within the probe into the corresponding intramolecular energy transition, in kcal mol^{-1}. Zwitterionic probes have been extensively employed because of their favorable UV–visible spectral properties. Examples include 2,6-diphenyl-4-(2,4,6-

---

**Correspondence to:* O. A. El Seoud, Instituto de Química, Universidade de São Paulo, C.P. 26077, 05513-970 São Paulo, S.P., Brazil.
E-mail: elseoud@iq.usp.br
Contact/grant sponsor: FAPESP.

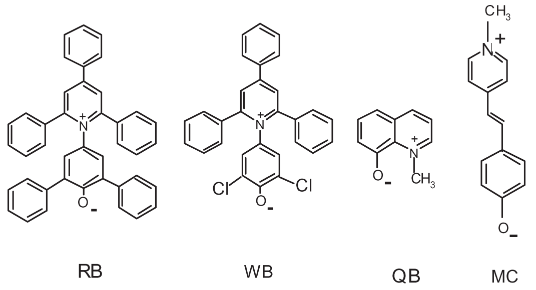

Figure 1. Structures of solvatochromic probes

triphenylpyridinium-1-yl)phenolate (RB), 2,6-dichloro-4-(2,4,6-triphenylpyridinium-1-yl)phenolate (WB), 1-methyl-8-oxyquinolinium betaine (QB) and 4-[2-(1-methylpyridinium-4-yl)ethenyl]phenolate (MC). Their structures are depicted in Fig. 1; the corresponding solvent polarity scales are designated $E_T(30)$, $E_T(33)$, $E_T(QB)$ and $E_T(MC)$, respectively.

Solvatochromic data have been analyzed by modeling the solvatochromic shift as a combination of a dipolarity/polarizability term, two hydrogen-bonding terms, in which the solvent is an H-bond donor or H-bond acceptor, and a cavity term.[5] Explanation of solvatochromic data in binary solvent mixtures is complex because of 'preferential solvation' of the probe by one component of the mixture. A significant consequence of this phenomenon is that the composition of the probe solvation microsphere is most probably different from that in bulk solvent.[4,6]

Thermo-solvatochromism refers to temperature-induced changes of solvatochromism. This phenomenon has been studied much less than solvatochromism, especially in binary solvent mixtures. The results can be employed, e.g., for calculation of the relative contributions of solvation barriers, and hence intrinsic energy barriers to the activation enthalpies of chemical reactions. A recently developed solvation model has been applied to analyze the thermo-solvatochromism of WB, QB and MC in binary mixtures of water with the following HBD solvents: methanol (MeOH), ethanol (EtOH), 1-propanol (1-PrOH), 2-propanol (2-PrOH), 2-methyl-2-propanol (2-Me-2-PrOH) and 2-methoxyethanol (MeOEtOH). The model is based on the presence, *in bulk solution*, of the solvents water (W), alcohol (ROH) and the 1:1 H-bonded species W–ROH (or W, ROEtOH and W–ROEtOH for mixtures of water with a 2-alkoxyethanol).[7]

We have now extended the range of 2-alkoxyethanols to include 2-ethoxyethanol (EtOEtOH), 2-*n*-propoxyethanol (PrOEtOH) and 2-*n*-butoxyethanol (BuOEtOH). In principle, the bifunctional structure of these solvents leads to the formation of several inter- and intramolecular H-bonded species, as discussed elsewhere.[8] Additionally, they are known to form clusters in aqueous solutions. In particular, BuOEtOH behaves as a short-chain non-ionic surfactant; several physical properties of its aqueous solution show a sudden variation at $\chi_{\mathrm{BuOEtOH}} \approx 0.05$ (χ refers to mole fraction); the homogeneous solution phase separates at ca 49 °C.[9,10] To our knowledge, thermo-solvatochromism has never been studied for mixtures of water with these 2-alkoxyethanols.

EXPERIMENTAL

Materials

The solvents (Acros and Merck) were purified by distillation from CaH_2 and stored over activated type 4 Å molecular sieves. Their purity was assured by comparing their experimentally determined $E_T(30)$ values (at 25 °C, where available) and densities (DMA 40 resonating-tube densimeter; Anton Paar, Graz, Austria) with literature values.[3b,11] The probes were available from previous studies.[7] Doubly distilled, deionized water was used throughout.

Sample preparation

Binary mixtures (16 per set) were prepared by weight at 25 °C. For MC, we employed a dilute aqueous solution of tetramethylammonium hydroxide (10^{-3} mol l^{-1}) instead of pure water, so that a convenient concentration of the probe zwitterionic form is always present.[7]

Spectrophotometric determination of E_T

The final probe concentration was $(2–5) \times 10^{-4}$ mol l^{-1}. No changes in λ_{max} and/or the peak shape were observed when the probe concentration was varied from 1×10^{-4} to 1×10^{-3} mol l^{-1}, indicating the absence of intermolecular probe interactions. We employed a Beckman DU-70 UV–visible spectrophotometer, provided with a thermostated cell holder (±0.05 °C). Each spectrum was recorded twice, at 120 nm min^{-1}; λ_{max} was determined from the first derivative of the absorption peak. The uncertainties in E_T are 0.1 kcal mol^{-1} for QB and ≤ 0.2 kcal mol^{-1} for WB and MC.

RESULTS AND DISCUSSION

The discussion is organized in the following order. First, we briefly discuss preferential solvation and the model that has been recently introduced in order to calculate the solvent fractionation factor, φ. We then address the dependence of φ on the properties of the organic solvent, the structure of the probe and temperature. Finally, temperature-induced desolvation is analyzed. Calculations of all quantities discussed are detailed in the Calculations section. In all ensuing discussion we use, for convenience, the symbol ROH to denote the organic solvent, alcohol and/or 2-alkoxyethanol.

Preferential solvation in binary solvent mixtures

In these mixtures, the dependence of E_T on solvent composition, e.g. on χ_W, is usually not linear because of ‘preferential solvation’ of the probe by one of the solvents present. In principle, this phenomenon includes contributions from dielectric enrichment and specific probe–solvent interactions, e.g. H-bonding. Non-linear behavior also results from solvent microheterogeneity, i.e. where solvent ‘clustering’ occurs.[3b,6,7] The realization that preferential solvation leads to differences between the compositions of bulk solvent and that in the solvation microsphere of the reaction has been employed in order to explain the (complex) dependence of reactivity on solvent composition.[12] Determination of the composition of the solvation microsphere is highly relevant, therefore, to the (correct) analysis of solvent effects on chemical phenomena.

The solvation model employed

The solvation model that we have recently introduced considers *explicitly* the formation of 1:1 H-bonded species between water and the HBD organic solvent. The formation of such species is manifested by several macroscopic and spectroscopic (IR and NMR) properties of these binary mixtures.[8,10,13–15] Equations (2)–(5) describe the solvent–exchange equilibria involved:[7]

$$\mathrm{ROH} + \mathrm{W} \rightleftharpoons \mathrm{ROH{-}W} \qquad (2)$$

$$\mathrm{Probe(ROH)}m + m\mathrm{W} \rightleftharpoons \mathrm{Probe(W)}_m + m\mathrm{ROH} \qquad (3)$$

$$\mathrm{Probe(ROH)}_m + m(\mathrm{ROH{-}W}) \rightleftharpoons \mathrm{Probe(ROH{-}W)}_m + m\mathrm{ROH} \qquad (4)$$

$$\mathrm{Probe(W)}_m + m(\mathrm{ROH{-}W}) \rightleftharpoons \mathrm{Probe(ROH{-}W)}_m + m\mathrm{W} \qquad (5)$$

where m is the number of solvent molecules whose exchange (in the solvation microsphere) affects E_T (usually $m \approx 1$). The most important consequence of this model is that the correlation between E_T and the medium composition is based on *effective*, not analytical concentrations of W and ROH. The relationship between bulk solvent composition and that in the probe solvation microsphere is given by the appropriate φs, defined by Eqns (6)–(8):

$$\varphi_{\mathrm{W/ROH}} = \frac{\chi_{\mathrm{W}}^{\mathrm{Probe}}/\chi_{\mathrm{ROH}}^{\mathrm{Probe}}}{\left(\chi_{\mathrm{W}}^{\mathrm{Bk;\,Effective}}/\chi_{\mathrm{ROH}}^{\mathrm{Bk,\,Effective}}\right)^{m}} \qquad (6)$$

$$\varphi_{\mathrm{ROH-W/ROH}} = \frac{\chi_{\mathrm{ROH-W}}^{\mathrm{Probe}}/\chi_{\mathrm{ROH}}^{\mathrm{Probe}}}{\left(\chi_{\mathrm{ROH-W}}^{\mathrm{Bk;\,Effective}}/\chi_{\mathrm{ROH}}^{\mathrm{Bk;\,Effective}}\right)^{m}} \qquad (7)$$

$$\varphi_{\mathrm{ROH-W/W}} = \frac{\chi_{\mathrm{ROH-W}}^{\mathrm{Probe}}/\chi_{\mathrm{W}}^{\mathrm{Probe}}}{\left(\chi_{\mathrm{ROH-W}}^{\mathrm{Bk;\,Effective}}/\chi_{\mathrm{W}}^{\mathrm{Bk;\,Effective}}\right)^{m}} \qquad (8)$$

where the superscript Bk refers to bulk solvent. For $\varphi_{\mathrm{W/ROH}} < 1$, the solvation microsphere is richer in ROH than bulk solvent; the converse is true for $\varphi_{\mathrm{W/ROH}} > 1$; $\varphi_{\mathrm{W/ROH}} = 1$ indicates an ideal behavior, i.e. the composition of the solvation microsphere and that of bulk solvent are the same. A similar line of reasoning applies to $\varphi_{\mathrm{ROH-W/ROH}}$ and $\varphi_{\mathrm{ROH-W/W}}$.

Dependence of thermo-solvatochromism on the properties of the probe, the organic HBD solvent and temperature

We now address the results of application of this model to the binary solvent mixtures studied. Where relevant, we include results for the previously studied ROH.[7] Analysis of our results leads to the following.

Table 1 shows K_{assoc} at different temperatures for the 2-alkoxyethanols studied. In all cases, the van’t Hoff equation was obeyed, i.e. the corresponding ΔC_p is essentially temperature independent in the temperature range studied, in agreement with published data.[16] K_{assoc} were then employed to calculate $\chi_{\mathrm{W}}^{\mathrm{Bk;\,Effective}}$, $\chi_{\mathrm{ROH}}^{\mathrm{Bk;\,Effective}}$ and $x_{\mathrm{ROH-W}}^{\mathrm{Bk;\,Effective}}$ respectively. The relationship between the analytical χ_W and effective mole fractions of the solvent components is shown in Fig. 2. ROH and W interact with each other by H-bonding, and hydrophobic hydration of the alkyl group, whereas hydrophobic interactions between the alkyl groups is the main force among ROH molecules. Table 2 shows the pK_a, McGowan’s intrinsic volume, V_X (a measure of alcohol hydrophobicity), and K_{assoc}, at 25 °C, for the nine HBD solvents studied. The pK_as of PrOEtOH and BuOEtOH were estimated, based on the difference between the pK_a of MeOEtOH and EtOEtOH (0.1 unit), and the known increase in the pK_a of aliphatic alcohols as a function of increasing length of R.[17] The fact that more basic alcohols do not bind more strongly to water shows that increasing the chain length of the alkyl group attenuates H-bonding, due to (a) an

Table 1. Density-based K_{assoc} at different temperatures for EtOEtOH–W, 1-PrOEtOH–W and 1-BuOEtOH–W

Binary mixture	Temperature (°C)	K_{assoc} (l mol^{-1})
EtOEtOH–W	10	13.0
	25	12.5
	40	12.1
	60	11.5
1-PrOEtOH–W	10	7.6
	25	7.0
	40	6.6
	60	6.1
1-BuOEtOH–W	10	5.0
	25	4.5
	40	4.0

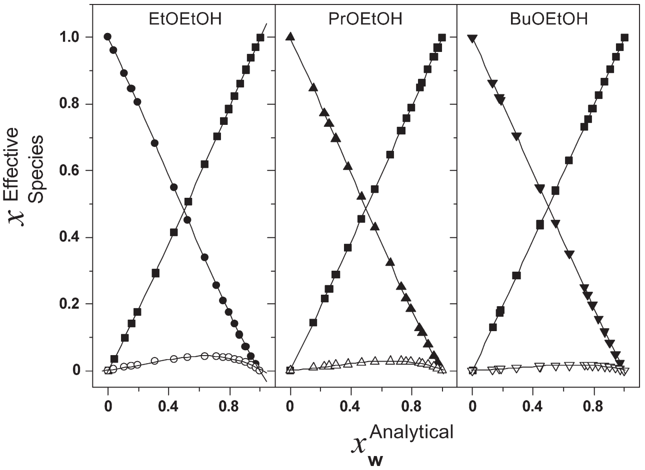

Figure 2. Species distribution at 25 °C, for EtOEtOH–W, PrOEtOH–W and BuOEtOH–W mixtures, respectively, W (■), EtOEtOH (●), PrOEtOH (▲), BuOEtOH (▼), EtOEtOH–W (○), PrOEtOH–W (△), and BuOEtOH–W (▽)

Table 2. Comparative data for all HBD solvents studied at 25 °C

HBD solvent	K_{assoc} $(l\,mol^{-1})^a$	$pK_a{}^d$	V_X $(cm^3\,mol^{-1}/100)^f$
MeOH	173.3[b]	15.5	0.308
EtOH	28.0[b]	15.9	0.449
1-PrOH	12.3[b]	16.1	0.590
2-PrOH	8.1[b]	17.1	0.590
2-Me-2-PrOH	7.0[b]	19.2	0.731
MeOEtOH	32.1[b]	14.8	0.649
EtOEtOH	12.5[c]	15.1	0.790
PrOEtOH	7.0[c]	15.2[e]	0.931
BuOEtOH	4.5[c]	15.3[e]	1.071

[a] K_{assoc} is the association constant of the 1:1 H-bonded complex between water and the organic HBD solvent.
[b] Data taken from Ref. 7.
[c] Data determined in the present work.
[d] Data taken from Ref. 18.
[e] Estimated values; see text for explanation.
[f] Calculated as given in Reference 19.

increase in hydrophobic interactions, whose relative importance increases rapidly as a function of increasing the volume of R and (b) an increase in the number of thermal collisions between W and ROH that are required for H-bond formation. The latter entails an increase in the time required for the alcohol molecule to assume a favorable orientation for H-bonding with water.[14,15,18] A similar explanation applies to 2-alkoxyethanols since their H-bonding occurs largely through the hydroxylic OH group.[14a,18b]

We calculated the (polynomial) dependence of E_T on the *analytical* χ_W and present the regression coefficients in Tables ESI-1 to ESI-3 (Electronic Supplementary Material, available in Wiley Interscience). The degree of the polynomial used is that which gave the best data fit, as indicated by the correlation coefficient, r^2, and the standard deviation, SD. The quality of our data is evidenced by these statistical parameters and by the excellent agreement between calculated and experimental $E_T(\text{probe})_{ROH}$ and $E_T(\text{probe})_W$, *at all temperatures*. At 25 °C, $E_T(\text{probe})_{ROH}$ and $E_T(\text{probe})_W$ are in excellent agreement with literature values (reported for EtOEtOH and BuOEtOH);[3,7] this agreement is an additional criterion for the purity of 2-alkoxyethanols.

$\chi_{\text{effective}}$ values of the species present are readily calculated from K_{assoc} and the densities of W and ROH at different temperatures, as given in the *Calculations* section. These mole fractions, and the data in Tables ESI-1 to ESI-3 (Electronic Supplementary Material) were employed to plot solvent polarity–temperature–solvent composition contours, as shown in Figs 3–5, for the probes studied in EtOEtOH and BuOEtOH.

The solvent fractionation factors shown in Table 3 were calculated from the appropriate E_T and $\chi_{\text{effective}}$. In discussing φ, it should be borne in mind that the zwitterionic form of the probe is the solvatochromic one, i.e. the probe acts as H-bond acceptor through its phenolate oxygen.[3b] There are also hydrophobic interactions between the probe and the alkyl chain of the organic solvent (either pure or as ROH–W). Therefore, preferential solvation is expected to depend on the pK_as and the hydrophilic/hydrophobic character of both the probe and ROH. All $\varphi_{W/ROH}$ were found to be <1, i.e. the probes are preferentially solvated by ROH, independent of their

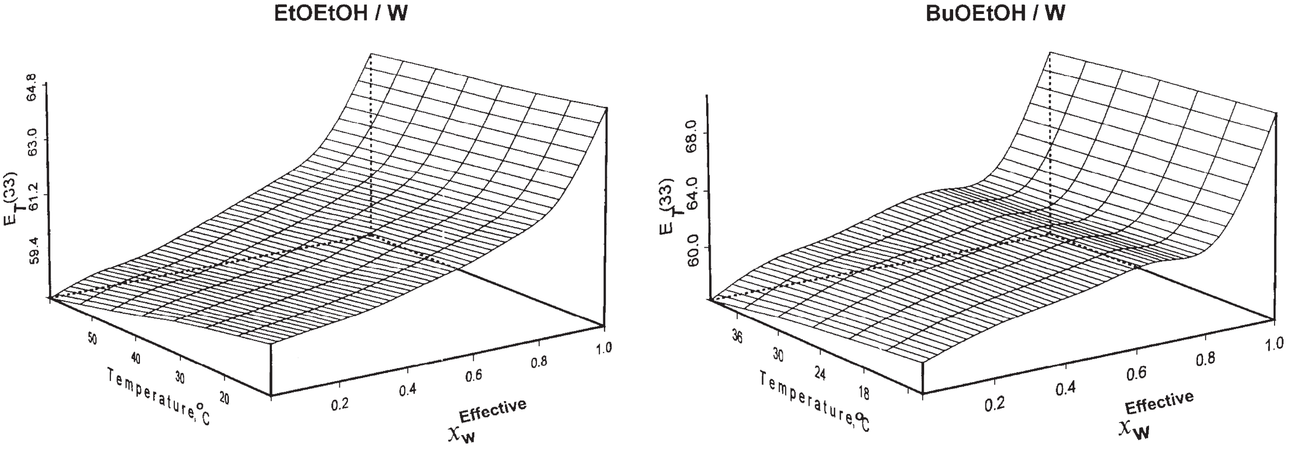

Figure 3. Solvent polarity–temperature–solvent composition contours for WB in EtOEtOH–W and BuOEtOH–W

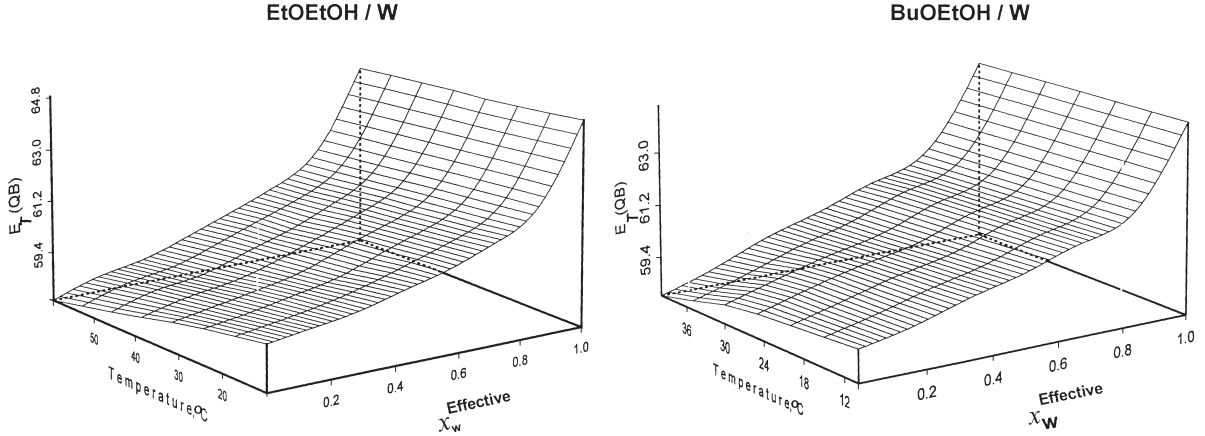

Figure 4. Solvent polarity–temperature–solvent composition contours for QB in EtOEtOH–W and BuOEtOH–W

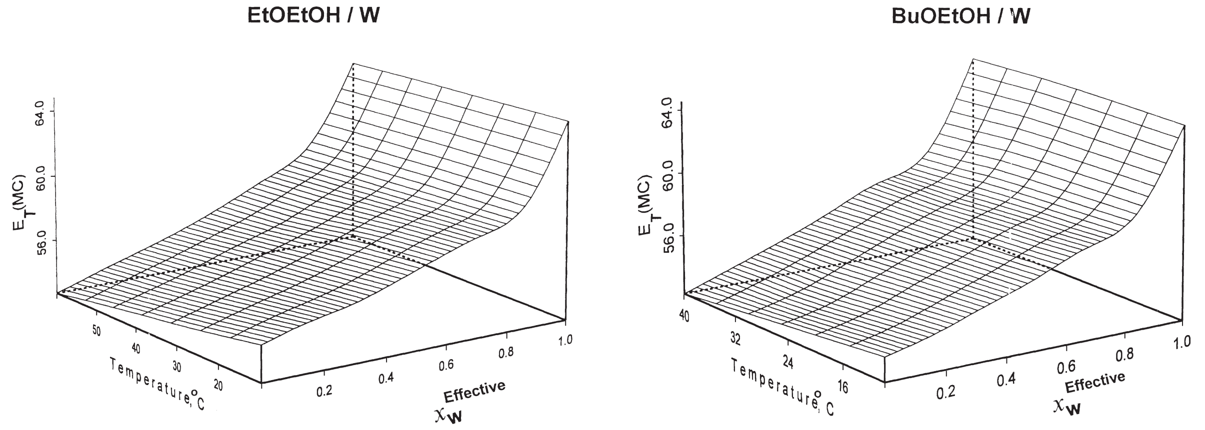

Figure 5. Solvent polarity–temperature–solvent composition contours for MC in EtOEtOH–W and BuOEtOH–W respectively

hydrophobicity. This seems to be a general behavior.[7] At each temperature, however, the observed order is $\varphi_{\mathrm{W/ROH}}(\mathrm{WB}) > \varphi_{\mathrm{W/ROH}}(\mathrm{QB})$ and $\varphi_{\mathrm{W/ROH}}(\mathrm{MC})$. The p$K_a$ values in water are 4.78, 6.80 and 8.37, whereas the log$P$ (a measure of hydrophobicity = log ([probe]$_{n\text{-octanol}}$/ [probe]$_{\mathrm{water}}$)[19] values are 1.79, −0.63 and −1.94, for WB, QB and MC, respectively.[7] That is, WB, the most hydrophobic and least basic probe, is less preferentially solvated by ROH (i.e. *more solvated by water*)! The reason is that the structure of WB enhances its H-bond acceptance, e.g. from water.[20] This probe is a derivative of 2, 6-dichlorophenol; the C—Cl bonds of chlorophenols are appreciably polarized, so that the chlorine atom forms H-bonds with suitable donors, e.g. HBD solvents.[21]

Table 3, and other recent data,[7b] show that *for each probe* the order of $\varphi_{\mathrm{W/ROH}}$ is MeOEtOH > EtOEtOH > PrOEtOH > BuEtOH; the single exception is WB at 40 °C, for which the order for MeOEtOH and EtOEtOH is reversed. That is, the longer the chain length of the 2-alkoxyethanol, the stronger its preferential solvation of the probe (small $\varphi_{\mathrm{W/ROH}}$ are associated with efficient solvation by ROH); an indication of the importance of probe–ROH hydrophobic interactions.

For 2-alkoxyethanols, in the temperature range studied, *all* $\varphi_{\mathrm{ROH\text{–}W/ROH}}$ and $\varphi_{\mathrm{ROH\text{–}W/W}}$ are >1, indicating that the probes are preferentially solvated by ROH–W. Likewise, *all* $\varphi_{\mathrm{ROH\text{–}W/W}}$ are larger than the corresponding $\varphi_{\mathrm{ROH\text{–}W/ROH}}$, indicating that ROH–W displaces water from the probe solvation microsphere more efficiently than 2-alkoxyethanol.

The order of *both* $\varphi_{\mathrm{ROH\text{–}W/ROH}}$ and $\varphi_{\mathrm{ROH\text{–}W/W}}$ is for each probe BuOEtOH > PrOEtOH > EtOEtOH > MeOEtOH (with one exception in 72 data points: WB in BuOEtOH, at 10 °C). That is, preferential solvation by ROH–W increases as a function of increasing the hydrophobicity of its HBD organic component. This conclusion agrees with the order of $\varphi_{\mathrm{W/ROH}}$ discussed above, and with the fact that $\varphi_{\mathrm{ROH\text{–}W/W}} > \varphi_{\mathrm{ROH\text{–}W/ROH}}$. This is because $\varphi_{\mathrm{ROH\text{–}W/W}}$ is related to the difference between H-bonding plus hydrophobic interactions of ROH–W versus only H-bonding by water [see Eqn (6)]. On the other hand, both H-bonding and hydrophobic interactions contribute to solvation by the two solvent components that define $\varphi_{\mathrm{ROH\text{–}W/ROH}}$.

We are interested in the dependence of φ on the properties of ROH. In order that our correlations are statistically meaningful,[5a,b] and considering that we have data for nine organic solvents, we decided to limit the number of properties (to be used in the correlation analysis) to two, namely ‘acidity’ and hydrophobicity of

Table 3. Analysis of thermo-solvatochromic responses in binary water–alcohol mixtures

ROH	Probe	T (°C)	m	$\varphi_{\mathrm{W/ROH}}$	$\varphi_{\mathrm{ROH–W/ROH}}$	$\varphi_{\mathrm{ROH–W/W}}$	$E_{\mathrm{T}}(\mathrm{probe})_{\mathrm{ROH}}$[a]	$E_{\mathrm{T}}(\mathrm{probe})_{\mathrm{W}}$[a]	SD[b]	ΣQ^2[b]
EtOEtOH	WB	10	1.532	0.378	55.137	145.865	59.471 [−0.051]	70.886 [0.034]	0.094	2.7×10^{-6}
		25	1.293	0.415	23.468	56.549	58.805 [−0.025]	70.531 [0.009]	0.068	2.8×10^{-6}
		40	1.157	0.587	19.261	32.813	57.766 [−0.006]	70.038 [0.007]	0.056	2.3×10^{-5}
		60	1.115	0.661	18.815	28.464	56.611 [−0.021]	69.290 [0.002]	0.071	3.1×10^{-6}
	QB	10	1.329	0.274	17.095	62.391	59.370 [−0.017]	64.850 [−0.010]	0.031	1.3×10^{-5}
		25	1.235	0.315	11.834	37.568	58.933 [0.005]	64.509 [0.003]	0.056	4.5×10^{-5}
		40	1.047	0.411	6.213	15.117	58.421 [−0.032]	64.291 [−0.004]	0.071	1.7×10^{-4}
		60	0.904	0.533	3.551	6.662	57.704 [−0.004]	63.955 [−0.006]	0.065	3.3×10^{-5}
	MC	10	1.314	0.251	20.610	82.112	55.071 [−0.140]	64.860 [−0.040]	0.105	2.8×10^{-6}
		25	1.188	0.288	13.106	45.507	54.234 [−0.045]	64.531 [−0.017]	0.079	1.2×10^{-4}
		40	1.021	0.367	6.273	17.093	53.547 [0.014]	64.238 [−0.015]	0.061	4.7×10^{-6}
		60	0.976	0.454	5.640	12.423	52.639 [0.029]	63.834 [−0.022]	0.109	4.6×10^{-5}
1-PrOEtOH	WB	10	1.382	0.221	63.003	285.081	59.414 [−0.174]	70.827 [0.047]	0.176	1.6×10^{-6}
		25	1.101	0.285	27.209	95.470	58.233 [−0.073]	70.322 [−0.042]	0.225	3.7×10^{-6}
		40	1.014	0.394	25.170	63.883	56.852 [−0.042]	69.764 [−0.024]	0.122	1.4×10^{-7}
		60	0.918	0.454	17.610	38.789	55.757 [−0.017]	69.210 [−0.023]	0.196	1.0×10^{-5}
	QB	10	1.194	0.163	17.252	105.840	59.252 [−0.010]	64.868 [0.002]	0.037	1.4×10^{-5}
		25	1.062	0.281	15.253	54.281	58.729 [−0.029]	64.696 [−0.009]	0.055	3.4×10^{-6}
		40	0.922	0.342	6.499	19.003	58.099 [0.001]	64.428 [0.004]	0.051	3.7×10^{-5}
		60	0.836	0.411	4.268	10.384	57.528 [−0.014]	64.111 [−0.004]	0.057	3.3×10^{-6}
	MC	10	1.278	0.211	47.227	223.825	54.369 [−0.109]	64.872 [−0.032]	0.129	2.7×10^{-6}
		25	1.052	0.250	17.330	69.320	53.550 [−0.089]	64.491 [−0.032]	0.128	1.8×10^{-5}
		40	0.933	0.313	9.230	29.489	52.771 [−0.037]	64.230 [−0.016]	0.081	9.7×10^{-6}
		60	0.896	0.361	7.099	19.665	51.943 [−0.006]	63.818 [−0.008]	0.088	1.0×10^{-5}
1-BuOEtOH	WB	10	1.067	0.173	60.567	350.098	58.370 [−0.050]	70.591 [−0.006]	0.086	1.2×10^{-6}
		25	0.992	0.192	56.440	293.958	57.470 [0]	70.153 [−0.010]	0.069	2.5×10^{-5}
		40	0.872	0.210	37.861	199.900	56.243 [−0.033]	69.502 [−0.002]	0.152	1.2×10^{-5}
	QB	10	1.074	0.171	23.540	137.661	59.172 [0.028]	64.629 [0.003]	0.034	7.2×10^{-6}
		25	0.990	0.238	16.459	69.155	58.868 [0.022]	64.421 [0.002]	0.065	2.1×10^{-5}
		40	0.891	0.291	13.267	45.591	58.026 [0.034]	64.173 [0.014]	0.095	1.5×10^{-6}
	MC	10	1.008	0.205	16.324	79.629	53.680 [0.009]	64.527 [0.023]	0.166	4.5×10^{-5}
		25	0.979	0.227	14.326	63.110	52.893 [0.107]	64.426 [0.037]	0.200	4.7×10^{-5}
		40	0.902	0.386	9.684	25.088	52.114 [0.084]	64.073 [0.052]	0.204	3.6×10^{-5}

[a] Calculated by regression of E_{T} of the binary mixture versus composition, and given in kcal mol^{-1}. The values in square brackets are $\Delta E_{\mathrm{T}}(\mathrm{probe})_{\mathrm{Solvent}}$ (ROH and/or W) = experimental $\Delta E_{\mathrm{T}}(\mathrm{probe})_{\mathrm{Solvent}}$ − calculated $\Delta E_{\mathrm{T}}(\mathrm{probe})_{\mathrm{Solvent}}$.

[b] SD = standard deviation; ΣQ^2 = sum of the squares of the residuals.

ROH.[3b,7] The same parameters have been employed to explain several properties of W–ROH binary mixtures, including density, relative permittivity, dielectric relaxation, NMR chemical shifts, IR frequency of the $\nu_{\mathrm{O–H}}$ band and formation of solvent 'clusters' in binary mixtures, as evidenced by mass spectrometry and as deduced from the Buff–Kirkwood integral functions.[13–22] The use of McGowan's intrinsic volume, V_{X} (cm^3 mol^{-1}/100), in structure–property relationships is superior to the corresponding bulk molar volume, because the latter also reflects the interactions between alcohol molecules in bulk liquid.[19] Solvent fractionation factors for all probes and organic solvents studied are listed in Table 4. The reason for reporting data at 25 °C is that pK_{a} and/or V_{X} are not available for other temperatures, and there are no established correlations between these properties and temperature. Modest correlation coefficients ($r^2 \leq 0.80$) were obtained for the regression analysis of $\varphi_{\mathrm{W/ROH}}$ versus (p$K_{\mathrm{a}} + V_{\mathrm{X}}$) for the three probes in the nine solvents studied. Since steric interactions affect the ability of ROH to form H-bonds,[22,23] we excluded the data for 2-PrOH and 2-Me-2-PrOH; this resulted in the equations.

$$\varphi_{\mathrm{W/ROH}}(\mathrm{WB}) = 3.332 - 0.163\,\mathrm{p}K_{\mathrm{a}} - 0.620\,V_{\mathrm{X}} \qquad r^2 = 0.8617 \tag{9}$$

$$\varphi_{\mathrm{W/ROH}}(\mathrm{QB}) = 1.020 - 0.0371\,\mathrm{p}K_{\mathrm{a}} - 0.193\,V_{\mathrm{X}} \qquad r^2 = 0.9834 \tag{10}$$

$$\varphi_{\mathrm{W/ROH}}(\mathrm{MC}) = 0.972 - 0.0343\,\mathrm{p}K_{\mathrm{a}} - 0.213\,V_{\mathrm{X}} \qquad r^2 = 0.9448 \tag{11}$$

If Eqns (9)–(11) are written as: φ = constant $-a\mathrm{p}K_{\mathrm{a}} - bV_{\mathrm{X}}$, then for each probe $|b| > |a|$; $|b|$ decreases in the order. WB > MC ≈ QB, i.e. in the same direction as the decrease in the hydrophobic character of the probes. A similar regression analysis was performed for $\varphi_{\mathrm{ROH–W/ROH}}$ and/or $\varphi_{\mathrm{ROH–W/W}}$ versus (p$K_{\mathrm{a}} + V_{\mathrm{X}}$).

Table 4. Calculated $\varphi_{W/ROH}$, $\varphi_{ROH\text{–}W/ROH}$ and $\varphi_{ROH\text{–}W/W}$ for all aqueous mixtures studied at 25 °C, and temperature-induced desolvation energies

Probe	ROH	$\varphi_{W/ROH}$	$\varphi_{ROH\text{–}W/ROH}$	$\varphi_{ROH\text{–}W/W}$	ΔE_T(solvent)/ΔT (cal mol^{-1} K^{-1})[a]	E_T(10 °C) − E_T (60 °C) (kcal mol^{-1})[b]
WB	MeOH	0.601	2.212	3.681	−48.4	
	EtOH	0.554	11.482	20.726	−46.2	2.1
	1-PrOH	0.265	149.208	563.049	−51.0	2.6
	2-PrOH	0.551	192.625	349.592	−44.7	2.4
	2-Me-2-PrOH	0.484	111.267	229.890	−68.0	
	MeOEtOH	0.479	5.659	11.814	−55.1	2.6
	EtOEtOH	0.415	23.468	56.549	−57.8	2.9
	PrOEtOH	0.285	27.209	95.470	−71.3	3.7
	BuOEtOH	0.192	56.440	293.958	−70.3	
QB	MeOH	0.381	1.172	3.076	−21.3	
	EtOH	0.349	5.053	14.479	−16.3	0.8
	1-PrOH	0.305	29.599	97.046	−21.0	1.1
	2-PrOH	0.428	26.418	61.724	−25.5	1.3
	2-Me-2-PrOH	0.364	21.713	59.651	−30.8	
	MeOEtOH	0.341	4.855	14.238	−27.3	1.4
	EtOEtOH	0.315	11.834	37.568	−33.4	1.7
	PrOEtOH	0.281	15.253	54.281	−34.9	1.7
	BuOEtOH	0.238	16.459	69.155	−38.0	
MC	MeOH	0.375	1.416	3.776	−39.5	
	EtOH	0.351	13.252	37.755	−41.7	2.2
	1-PrOH	0.274	23.279	84.960	−49.4	2.5
	2-PrOH	2.918	105.188	36.048	−41.2	2.1
	2-Me-2-PrOH	0.554	18.283	33.002	−23.1	
	MeOEtOH	0.318	6.888	21.660	−47.2	2.4
	EtOEtOH	0.288	13.106	45.507	−45.1	2.4
	PrOEtOH	0.250	17.330	69.320	−46.4	2.4
	BuOEtOH	0.227	14.326	63.110	−52.4	

[a] ΔE_T(W) are 31 ± 3, 17 ± 3 and 19 ± 2 cal mol^{-1} K^{-1} for WB, QB and MC, respectively.

[b] The values for water are 1.6, 0.9 and 1.0 kcal mol^{-1} for WB, QB and MC, respectively.

Although the correlation coefficients obtained were lower than those calculated for $\varphi_{W/ROH}$ ($r^2 = 0.57$–0.77 and 0.64–0.92, respectively), the trends observed were the same. This lack of better correlations may be attributed to the fact that the parameters employed in the regression analyses (i.e. pK_a and V_X) were those of the precursor ROH, not of the (experimentally inaccessible) complex species ROH–W. The relevant point is that H-bond donation by ROH to the phenolate oxygen of the probe and probe–solvent hydrophobic interactions seem to be the major factors that affect solvation of these indicators and, presumably, other species (reactants and activated complexes) for which they serve as models.

We now focus on the relevance of thermo-solvatochromism for a clearer understanding of the role of solvation in chemical reactions. In doing so, we address the following points: (a) response of the probes to composition-induced structural changes in the binary solvent mixture and (b) effects of temperature on solvation. Point (a) is shown in Fig. 6, which depicts the dependence of reduced E_T, $E_T^r = \left(E_T^{obs} - E_T^{ROH}\right)/\left(E_T^{W} - E_T^{ROH}\right)$, on χ_W, for the water-rich regions of aqueous methanol and aqueous BuOEtOH. In the former binary mixture, E_T increases gradually as a function of increasing χ_W, whereas the change is abrupt for aqueous BuOEtOH, especially at the 'magic' χ_{ROH}, 0.05. As was indicated above, this is the composition at which solution properties change abruptly and, as a consequence, the activation enthalpy and entropy of several pH-independent hydrolytic reactions show maxima and minima.[9,10,24] This shows that the probes employed respond to changes of the intermolecular structures of binary solvent mixtures

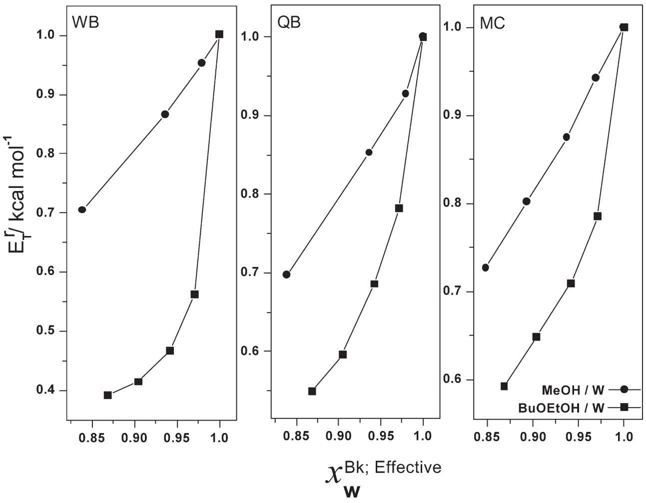

Figure 6. Dependence of reduced E_T on water mole fraction, χ_W for the water-rich regions of aqueous methanol and aqueous BuOEtOH, for WB, QB and MC

that accompany changes in their compositions,[25a] i.e. the probes serve as models for chemical reactions. Point (b) includes effects of temperature on solvation by pure solvents (W and/or ROH) and binary solvent mixtures. Table 3 shows that as the temperature increases, m, $E_T(\text{probe})_{\text{ROH}}$, $E_T(\text{probe})_{\text{W}}$, $\varphi_{\text{ROH–W/ROH}}$ and $\varphi_{\text{ROH–W/W}}$ *decrease*, whereas $\varphi_{\text{W/ROH}}$ *increases*. The decrease in the polarities of pure solvents can be attributed to a decrease in solvent stabilization of the probe ground state, as a result of the concomitant decrease in solvent structure, and H-bonding ability.[25] Preferential 'clustering' of water and ROH as a function of increasing temperature means that the strength of ROH–W interactions also decreases as a function of increasing temperature,[13b,c,25,26] with a concomitant decrease in the ability of the mixed species to displace both water and alcohol. This explains the decrease in $\varphi_{\text{ROH–W/ROH}}$ and $\varphi_{\text{ROH–W/W}}$ with increase in temperature. Plots (not shown) of $E_T(\text{probe})_{\text{Solvent}}$ versus T gave excellent straight lines ($r^2 \geq 0.99$ for 90% of the data), whose (negative) slopes are given by $\Delta E_T(\text{probe})_{\text{Solvent}}/\Delta T$ ($\text{cal mol}^{-1}\,\text{K}^{-1}$). These were calculated for all pure solvents and are listed in Table 4. The order is $|\Delta E_T(\text{probe})_{\text{ROH}}| > |\Delta E_T(\text{probe})_{\text{W}}|$, reflecting the greater effect of temperature on the structure of ROH. Consequently, H-bonding of water with the probe ground state is less susceptible to temperature increase than its ROH counterpart. This leads to a measurable 'depletion' of ROH in the probe solvation microsphere, so that $\varphi_{\text{W/ROH}}$ increases as a function of increasing temperature.[7] With regard to the contribution of desolvation energy to $\Delta H^{\neq}$, consider a chemical reaction for which the solvatochromic transition of WB serves as a model, e.g. pH-independent hydrolyses of 1-acyl-1,2,4-triazoles, 4-methoxyphenyl 2,2-dichloropropionate and bis(2,4-dinitrophenyl) carbonate. Table 3 and previous data show that $E_T(10\,°\text{C}) - E_T(60\,°\text{C})$ ranges between 2.1 and $3.7\,\text{kcal mol}^{-1}$, whereas $\Delta H^{\neq}$ for the above-mentioned reactions range from 7.8 to $13.5\,\text{kcal mol}^{-1}$.[27]

That is, temperature-induced desolvation is sizeable, accounting for 15–47% of the reaction activation enthalpies! This underlines the importance of studying thermo-solvatochromism to quantify the contribution of temperature-induced changes in solvation to the energetics of reactions in solution, a quantity that cannot be calculated, e.g. from rate data.

Finally, a brief discussion of the composition scale employed is in order, because it affects the fractionation factors calculated. Compositions of mixtures may be described in terms of their molarities, molalities, volume fractions, VF ($V_W/V_W + V_{\text{ROH}}$), and/or mole fractions. Because the temperature range employed in the present study is rather wide (10–60 °C), it is advisable to employ a temperature-independent scale, i.e. molarity and VF are not convenient, because the coefficients of thermal expansivity of liquids is both temperature and solvent dependent. The temperature-independent molality scale is based on the number of moles of a solute per kilogram of solvent. The meaning of solute and solvent becomes unclear in the present case, because χ_W varies from 0 to 1. That is, if ROH is considered the solvent over the entire composition range, then the molality scale becomes open-ended, because the number of moles of water per kilogram of ROH becomes progressively large. Additionally, in order to convert Eqn (23) (see Calculations section) to this scale, the molality of each species present, W, ROH and ROH–W, should be known. If alcohol is chosen as the solvent, then only the molality of W and ROH–W can be calculated. That the mole fraction is the most important quantity, as far as the laws of mixing of components are concerned, is evidenced by its use in the definition of the chemical potential and the standard states of solutes in solutions. It is also employed in equations that describe the behavior of multi-component systems, e.g. Gibbs–Duhem and Duhem–Margules equations, and in describing the dependence of macroscopic and spectroscopic properties of mixtures on their composition[28] (see 'Note on composition scales' and attached references, in Electronic Supplementary Material). In order to show the importance of the composition scale employed, we have plotted $E_T(\text{RB})$, at 25 °C, as a function of χ_W and/or VF of water for aqueous solutions of 1-PrOH and 2-Me-2PrOH, respectively (Fig. 1, Electronic Supplementary Material). Whereas the former scale shows preferential solvation by ROH (for both solvents), the latter shows the converse! This is an intriguing result in view of the large body of data that indicates that RB is preferentially solvated by the organic component of the aqueous mixture,[7,20,25,29] in agreement with its negligible solubility in water, $2 \times 10^{-6}\,\text{mol l}^{-1}$.[3b] In summary, the basic thermodynamic equations that describe the behavior of multi-component systems, and the large body of data on the macroscopic, spectroscopic and solvatochromic properties of binary solvent mixture, rely on the mole fraction scale.

CONCLUSIONS

Thermo-solvatochromism can be described by a model based on exchange equilibria between the species present in solution (W, ROH, ROH–W) with ROH and/or W present in the probe solvation microsphere. Analysis of all data available, five aliphatic alcohols and four 2-alkoxyethanols, indicated that the different φs can be rationalized in terms of H-bonding and hydrophobic interactions, the latter being more important. Temperature increase results in gradual desolvation of every probe. Desolvation energies depend on the molecular structures of the probe and the solvent and are sensitive to the composition of the binary solvent mixture. The relevance of these results to reactions for which solvatochromic probes serve as models is that they can be employed to quantify the contribution of desolvation energies to the corresponding enthalpies of activation.

CALCULATIONS

Determination of K_{assoc} and $\chi^{\mathrm{Effective}}_{\mathrm{Species}}$ from density data

The model proposed by Katz and co-workers[30] has been employed to determine the association constant of W and ROH from density data. The model is based on the formation of a 1:1 ROH–W complex, Eqn (2), whose dissociation constant, K_{dissoc} is given by Eqn (12):

$$K_{\mathrm{dissoc}} = \frac{[\mathrm{ROH}][\mathrm{W}]}{[\mathrm{ROH{-}W}]} \tag{12}$$

where K_{assoc} is the reciprocal of K_{dissoc}. The density of a solution composed of W, ROH, and ROH–W is given by Eqn (13):

$$d = \frac{[\mathrm{W}]M_{\mathrm{W}} + [\mathrm{ROH}]M_{\mathrm{ROH}} + [\mathrm{ROH{-}W}]M_{\mathrm{ROH-W}}}{[\mathrm{W}]V_{\mathrm{W}} + [\mathrm{ROH}]V_{\mathrm{ROH}} + [\mathrm{ROH{-}W}]V_{\mathrm{ROH-W}}} \tag{13}$$

where [W], [ROH], [ROH–W], M and V refer to molar concentration, molecular mass and molar volume of the appropriate species, respectively. [W], [ROH] and [ROH–W] are given by Eqns (14)–(16):

$$[\mathrm{W}] = \frac{-b + (b^2 + 4c)^{0.5}}{2} \tag{14}$$

$$[\mathrm{ROH}] = \frac{VF(\mathrm{ROH})}{V_{\mathrm{ROH}}} - [\mathrm{ROH{-}W}] \tag{15}$$

$$[\mathrm{ROH{-}W}] = \frac{1 - VF(\mathrm{ROH})}{V_{\mathrm{W}}} - [\mathrm{W}] \tag{16}$$

where VF(ROH) is the analytical volume fraction of ROH and the coefficients b and c of Eqn (14) are given by

$$b = K_{\mathrm{dissoc}} + \frac{VF(\mathrm{ROH})}{V_{\mathrm{ROH}}} + \frac{VF(\mathrm{ROH})}{V_{\mathrm{W}}} - \frac{1}{V_{\mathrm{W}}} \tag{17}$$

$$c = K_{\mathrm{dissoc}}\left[\frac{1}{V_{\mathrm{W}}} - \frac{VF(\mathrm{ROH})}{V_{\mathrm{W}}}\right] \tag{18}$$

The input data to solve Eqn (13) include M_{W}, M_{ROH}, $M_{\mathrm{ROH\text{–}W}}$, V_{M} and V_{ROH}, along with initial estimates for K_{dissoc} and $V_{\mathrm{ROH\text{–}W}}$. The densities were calculated by iteration as described previously.[7] We have determined the densities of EtOEtOH/W and PrOEtOH/W in the range 25–50 °C and of BuOEtOH/W in the range 25–45 °C. As shown by the following regression analysis, the van't Hoff equation applied satisfactorily to the data and was employed to obtain K_{assoc} at the desired temperatures (see Table 1). Figure 7 shows typical results, where the densities are experimental and the curves were obtained by iteration.

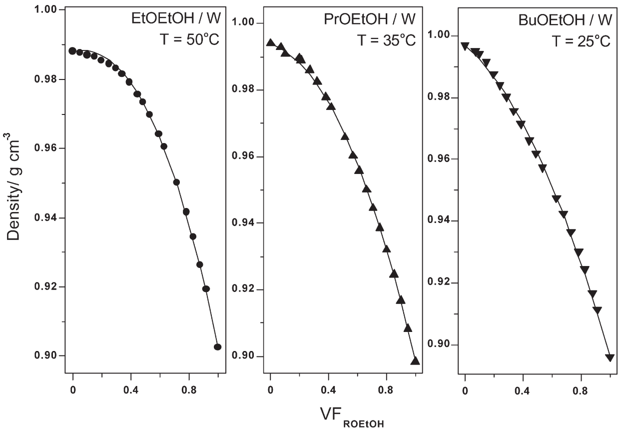

Figure 7. Representative plots showing the dependence of calculated and experimental solution density on the 2-alkoxyethanol volume fraction, *VF*, in aqueous EtOEtoH, PrOEtoH and BuOEtOH. The points are experimental and the curves were generated from Eqn (13) by iteration

$$\text{EtOEtOH/W:}\quad \ln K_{\mathrm{assoc}} = 226.967\,\mathrm{T}^{-1} - 1.765 \qquad r = 0.9985 \tag{19}$$

$$\text{PrOEtOH/W:}\quad \ln K_{\mathrm{assoc}} = 417.175\,\mathrm{T}^{-1} + 0.555 \qquad r = 0.9936 \tag{20}$$

$$\text{BuOEtOH/W:}\quad \ln K_{\mathrm{assoc}} = 631.025\,\mathrm{T}^{-1} - 0.615 \qquad r = 0.9952 \tag{21}$$

Preferential solvation model

The probe solvation microsphere is composed of W, ROH and ROH–W. The observed E_{T}, $E_{\mathrm{T}}^{\mathrm{obs}}$, is the sum of the polarity of each component, $E_{\mathrm{T}}^{\mathrm{W}}$, $E_{\mathrm{T}}^{\mathrm{ROH}}$ and $E_{\mathrm{T}}{}^{\mathrm{ROH-W}}$, multiplied by the corresponding mole fraction in the probe solvation microsphere, $\chi_{\mathrm{W}}^{\mathrm{Probe}}$, $\chi_{\mathrm{ROH}}^{\mathrm{Probe}}$ and $\chi_{\mathrm{ROH-W}}^{\mathrm{Probe}}$, respectively:

$$E_{\mathrm{T}}^{\mathrm{obs}} = \chi_{\mathrm{W}}^{\mathrm{Probe}} E_{\mathrm{T}}^{\mathrm{W}} + \chi_{\mathrm{ROH}}^{\mathrm{Probe}} E_{\mathrm{T}}^{\mathrm{ROH}} + \chi_{\mathrm{ROH-W}}^{\mathrm{Probe}} E_{\mathrm{T}}^{\mathrm{ROH-W}} \tag{22}$$

Substitution of Eqns (6) and (7) in Eqn (22) gives Eqn (23):

$$E_{\mathrm{T}}^{\mathrm{obs}} = \frac{\left(\chi_{\mathrm{ROH}}^{\mathrm{Bk;\,Effective}}\right)^m E_{\mathrm{T}}^{\mathrm{ROH}} + \varphi_{\mathrm{W/ROH}}\left(\chi_{\mathrm{W}}^{\mathrm{Bk;\,Effective}}\right)^m E_{\mathrm{T}}^{\mathrm{W}} + \varphi_{\mathrm{ROH-W/ROH}}\left(\chi_{\mathrm{ROH-W}}^{\mathrm{Bk;\,Effective}}\right)^m E_{\mathrm{T}}^{\mathrm{ROH-W}}}{\left(\chi_{\mathrm{ROH}}^{\mathrm{Bk;\,Effective}}\right)^m + \varphi_{\mathrm{W/ROH}}\left(\chi_{\mathrm{W}}^{\mathrm{Bk;\,Effective}}\right)^m + \varphi_{\mathrm{ROH-W/ROH}}\left(\chi_{\mathrm{ROH-W}}^{\mathrm{Bk;\,Effective}}\right)^m} \tag{23}$$

where $\chi_{\mathrm{W}}^{\mathrm{Probe}} + \chi_{\mathrm{ROH}}^{\mathrm{Probe}} + \chi_{\mathrm{ROH-W}}^{\mathrm{Probe}} = 1$; (m), $\chi_{\mathrm{ROH}}^{\mathrm{Bk;\,Effective}}$, $x_{\mathrm{W}}^{\mathrm{Bk;\,Effective}}$ and $x_{\mathrm{ROH-W}}^{\mathrm{Bk;\,Effective}}$ refer to the number of solvent molecules in the micro-sphere that affect the solvatochromic response, and effective mole fractions of the appropriate species in bulk solvent, respectively. The input data to solve Eqn (23) include $E_{\mathrm{T}}^{\mathrm{obs}}$, $E_{\mathrm{T}}^{\mathrm{W}}$, $E_{\mathrm{T}}^{\mathrm{ROH}}$ and $\chi_{\mathrm{Species}}^{\mathrm{Effective}}$, along with initial estimates of m, $E_{\mathrm{T}}^{\mathrm{ROH-W}}$ and the appropriate φ. The solvent fractionation factor, $\varphi_{\mathrm{ROH-W/W}}$, is obtained from the ratio between $\varphi_{\mathrm{ROH-W/ROH}}$ and $\varphi_{\mathrm{ROH/W}}$. $E_{\mathrm{T}}^{\mathrm{obs}}$ was calculated by iteration until ΣQ^2 was $\leq 10^{-3}$. Calculations were based on a home-developed BASIC script that relies on the S-Plus 2000 program package (MathSoft, Seattle, WA, USA).

Acknowledgements

We thank FAPESP (State of São Paulo Research Fountaion) for financial support and a pre-doctoral research fellowship to E. B. Tada, CNPq (National Council for Scientific and Technological Research) for a research productivity fellowship to O. A. El Seoud and a BIPIC fellowship to P. L. Silva, and C. Guizzo for his help. We thank Professor T. W. Bentley for sending us his submitted paper regarding the composition scales of binary mixtures.

REFERENCES

1. (a) Kemp DS, Paul KG. *J. Am. Chem. Soc.* 1975; **97**: 7305–7312; (b) Kemp DS, Reczek J, Vellaccio F. *Tetrahedron Lett.* 1978; **8**: 741–742.
2. Carey FA, Sundberg RJ. *Advanced Organic Chemistry, Part A* (4th edn). Kluwer/Plenum: New York, 2000; 263, and references cited therein.
3. (a) Reichardt C. *Solvents and Solvent Effects in Organic Chemistry* (3rd edn). VCH: Weinheim, 2003; (a) 147; (b) 389, and references cited therein; (b) Reichardt C, Röchling A, Schäfer G. *J. Phys. Org. Chem.* 2003; **16**: 682–690.
4. Dewar MJS, Storch DM. *J. Chem. Soc., Perkin Trans. 2* 1989; 877.
5. (a) Kamlet MJ, Abboud J-LM, Taft RW. *Prog. Phys. Org. Chem.* 1981; **13**: 485–630; (b) Abraham MH, Grellier PL, Abboud J-LM, Doherty RM, Taft RW. *Can. J. Chem.* 1988; **66**: 2673–2686; (c) Laurence C, Nicolet P, Dalati MT, Abboud J-LM, Notario R. *J. Phys. Chem.* 1994; **98**: 5807–5816.
6. Suppan P, Ghoneim N. *Solvatochromism*. Royal Society of Chemistry: Cambridge, 1997; 21, and references cited therein.
7. (a) Tada EB, Silva PL, El Seoud OA. *J. Phys. Org. Chem.* 2003; **16**: 691–699; (b) Tada EB, Silva PL, El Seoud OA. *Phys. Chem. Chem. Phys*. 2003; **5**: 5378–5385.
8. Brinkley RL, Gupta RB. *Ind. Eng. Chem. Res.* 1998; **37**: 4823–4827.
9. (a) Roux G, Perron G, Desnoyers JE. *J. Solution Chem.* 1978; **7**: 639–654; (b) Quirion F, Magid LJ, Drifford M. *Langmuir* 1990; **6**: 244–249; (c) Koehler RD, Schubert K-V, Strey R, Kaler EW. *J. Chem. Phys.* 1994; **101**: 10843–10849; (d) D'Angelo M, Onori G, Santucci A. *Chem. Phys. Lett.* 1994; **220**: 59–63; (e) Onori G, Santucci A. *J. Phys. Chem. B* 1997; **101**: 4662–4666.
10. (a) Ito N, Saito K, Kato T, Fujiyama T. *Bull. Chem. Soc. Jpn.* 1981; **54**: 991–997; (b) Ito N, Fujiyama T, Udagawa Y. *Bull. Chem. Soc. Jpn.* 1983; **56**: 379; (c) D'Arrigo G, Mallamace F, Micali N, Paparelli A, Vasi C. *Phys. Rev. A* 1991; **44**: 2578–2587.
11. Shindo Y, Kusano K. *J. Chem. Eng. Data* 1979; **24**: 106–110.
12. (a) El Seoud OA, El Seoud MI, Farah JPS. *J. Org. Chem.* 1997; **62**: 5928–5933; (b) Humeres E, Nunes RJ, Machado VG, Gasques MDG, Machado C. *J. Org. Chem.* 2001; **66**: 1163–1170; (c) Wakisaka A, Komatsu S, Usui Y. *J. Mol. Liq.* 2001; **90**: 175–184; (d) Mancini PM, Terenzani A, Adam C, Vottero LR. *J. Phys. Org. Chem.* 1999; **12**: 430–440; (e) Mancini PM, Adam C, Del A, Pérez C, Vottero LR. *J. Phys. Org. Chem.* 2000; **13**: 221–231.
13. (a) Marcos Y. *Chem. Soc. Rev.* 1993; **22**: 409–416; (b) Shulgin I, Rukenstein E. *J. Phys. Chem. B* 1999; **103**: 872–877; (c) Marcus Y. *Monatsh. Chem.* 2001; **132**: 1387–1411.
14. (a) Kaatze U, Pottel R, Schumacher A. *J. Phys. Chem.* 1992; **96**: 6017–6020; (b) Brai M, Kaatze U. *J. Phys. Chem.* 1992; **96**: 8946–8955; (c) Kaatze U, Schumacher A, Pottel R. *Ber. Bunsenges. Phys. Chem.* 1991; **95**: 585–592; (d) Petong P, Pottel R, Kaatze U. *J. Phys. Chem. A* 2000; **104**: 7420–7428.
15. (a) Chen J-S, Shiao J-C. *J. Chem. Soc., Faraday Trans.* 1994; **90**: 429–433; (b) Eblinger F, Schneider H-J. *J. Phys. Chem.* 1996; **100**: 5533–5537.
16. (a) Kusano K, Suurkkusk J, Wadsö I. *J. Chem. Thermodyn.* 1973; **5**: 757–767; (b) Davis MI, Molina MC, Douhéret G. *Thermochim. Acta* 1998; **317**: 105; (c) Tamura K, Tabata S, Murakami S. *J. Chem. Thermodyn.* 1998; **30**: 1319–1332.
17. (a) Barlin GB, Perrin DD. *Q. Rev. Chem. Soc.* 1966; **20**: 75–101; (b) Takahashi S, Cohen LA, Miller HK, Peake EG. *J. Org. Chem.* 1971; **36**: 1205–1209.
18. (a) Max J-J, Daneault S, Chapados C. *Can. J. Chem.* 2002; **80**: 113–123; (b) Michale MER, Coym KS, Roy LE, Hernández CE, Acree WE Jr. *Can. J. Chem.* 1997; **75**: 1403–1408.
19. (a) Abraham MH, McGowan JC. *Chromatographia* 1987; **23**: 243–246; (b) Abraham MH. *Chem. Soc. Rev.* 1990; 73–83.
20. (a) Tada EB, Novaki LP, El Seoud OA. *J. Phys. Org. Chem.* 2000; **13**: 679–687; (b) Antonius MS, Tada EB, El Seoud OA. *J. Phys. Org. Chem.* 2002; **15**: 403–412.
21. Chandramani R, Devaraj N. *J. Chem. Soc., Faraday Trans. 2* 1980; **76**: 1055–1060.
22. (a) Kingston B, Symons MCR. *J. Chem. Soc. Farady Trans. 2* 1973; **69**: 978–992; (b) Symons MCR. *Pure Appl. Chem.* 1986; **58**: 1121–1132.
23. Coleman CA, Murray CJ. *J. Org. Chem.* 1992; **57**: 3578–3582.
24. (a) Engberts JBFN. *Pure Appl. Chem.* 1982; **54**: 1797–1808, and references cited therein; (b) Blokzijl W, Engberts JBFN, Jager J, Blandamer MJ. *J. Phys. Chem.* 1987; **91**: 6022–6027; (c) Blokzijl W, Blandamer MJ, Engberts JBFN. *J. Org. Chem.* 1991; **56**: 1832–1837; (d) Buurma NJ, Pastorello L, Blandamer MJ, Engberts JBFN. *J. Am. Chem. Soc*. 2001; **123**: 11848–11853.
25. (a) Haak JR, Engberts JBFN. *Recl. Trav. Chim. Pays-Bas* 1986; **105**: 307–311; (b) Zana R, Eljebari MJ. *Recl. Trav. Chim. Pays-Bas* 1993; **97**: 11134–11136; (c) Guillaume YC, Guinchard C. *Anal. Chem.* 1998; **70**: 608–615; (d) Harris KR, Newitt PJ. *J. Phys. Chem. A* 1999; **103**: 6508–6513.
26. (a) Nishikawa K, Hayashi H, Iijima T. *J. Phys. Chem.* 1989; **93**: 6559–6565; (b) Huelskopf M, Ludwig R. *J. Mol. Liq.* 2000; **85**: 105–125.
27. (a) Holterman HAJ, Engberts JBFN, Blandamer MJ. *J. Am. Chem. Soc.* 1982; **104**: 6382–6384; (b) Haak JR, Engberts JBFN, Blandamer MJ. *J. Am. Chem. Soc.* 1985; **170**: 6031–6035; (c) Possidonio S, El Seoud AO. *J. Mol. Liq.* 1999; **80**: 231–251.
28. (a) Kothoff IM, Elving PJ. *Treatise on Analytical Chemistry.* Interscience: New York, 1959; 233; (b) Murrell JN, Jenkins AD. *Properties of Liquids and Solutions*. Wiley: New York, 1994; 102; (c) Marcus Y. *The Properties of Solvents*. Wiley: New York, 1988; 34; (d) Berry RS, Rice SA, Ross J. *Physical Chemistry.* Wiley: New York, 1980; 680, 901.
29. (a) Ortega J, Ràfols C, Bosch E, Roses M. *J. Chem. Soc., Perkin Trans. 2* 1996; 1497–1503; (b) Rosés M, Buhvestov U, Ràfols C, Rived F, Bosch E. *J. Chem. Soc., Perkin Trans. 2* 1997; 1341–1348; (c) Buhvestov U, Rived F, Ràfols C, Bosch E, Rosés M. *J. Phys. Org. Chem.* 1998; **11**: 185–192; (d) Das PK, Pramanik R, Bagchi S. *Spectrochim. Acta, Part A* 2003; **59**: 1681–1688.
30. (a) Katz ED, Ogan K, Scott RPW. *J. Chromatogr.* 1986; **352**: 67–90; (b) Katz ED, Lochmüller CH, Scott RPW. *Anal. Chem.* 1989; **61**: 349–355.